IEEE Access
Multidisciplinary | Rapid Review | Open Access Journal

Received 18 June 2022, accepted 20 July 2022, date of publication 26 July 2022, date of current version 4 August 2022.

Digital Object Identifier 10.1109/ACCESS.2022.3193942

METHODS

Automatic Expansion of Voltage Signals Using Empirical Mode Decomposition for Voltage Sag Detection

HEYANG LI, CHAO MENG, (Member, IEEE), AND YINGRU ZHAO
College of Energy, Xiamen University, Xiamen 361000, China

Corresponding author: Chao Meng (meng@xmu.edu.cn)

This work was supported in part by the National Natural Science Foundation of China, and in part by the Xiamen Municipal Science and Technology Bureau-Xiamen City Division of Fund Management Project.

ABSTRACT Voltage sag is one of the most harmful power quality issues. In practical engineering, harmonic and noise interference problems will bring big challenges to the analysis of voltage signals. These disturbances can easily lead to a delay or even false detection of the voltage signal. To address this problem, adaptive processing and diagnosis methods of the voltage signal, such as the Empirical Mode Decomposition (EMD) and the Variational Mode Decomposition (VMD), have become a research hotspot. In order to overcome the interference of voltage harmonic and achieve rapid voltage sag detection, this paper first analyzes the performance of EMD and VMD in decomposing voltage sag signals. Then, a tailored EMD-based adaptive voltage signal expansion method for real-time voltage sag detection is proposed. The sampling voltage signal is automatically expanded using the real-time voltage signal to achieve the rapid detection of voltage sag under complex operational environments. Numerical results demonstrate that the proposed method can detect the voltage sag within 1 millisecond.

INDEX TERMS Power quality, voltage sag, tailored empirical mode decomposition, Hilbert transform.

I. INTRODUCTION

The power quality problems have plagued industrial production for a long time. With the rapid development of the social output, power quality problems have become the focus of public attention. Intermittent distributed generation, nonlinear loads, and various power electronic devices make power quality problems the main challenges for power grids. At the same time, with the rapid development of computer and digital technology, intelligent control technology, precision machining, manufacturing technology, and related industries, more sensitive loads have appeared in the power grid, which has caused the importance of power quality issues to become increasingly prominent [1].

The voltage sag problem is one of the most severe power quality problems [2], [3]. Power quality management devices, such as Dynamic Voltage Regulator (DVR) and Uninterrupted Power Supply (UPS), will often be used to solve voltage sag. The transient disturbance detection and identification technology is the prerequisite for achieving voltage sag treatment. Recently, some researches [4] and [5] focus on voltage sag detection, but the identification time is usually within 5ms. For conventional loads, this detection time is acceptable. While for precision loads, such as MOCVD and lithography machines, this detection time is too long. It is particularly crucial to achieving real-time monitoring and analysis of voltage signals. Meanwhile, the voltage harmonics also significantly impact the effectiveness of voltage sag detection. Therefore, a fast and effective signal processing method is necessary to extract fault information from voltage signals [6]–[8].

Based on the requirements above, various signal processing tools have been proposed in many documents, which can be used for automatic anomaly detection and fault feature extraction of the voltage signal. Among these detection methods, the Root-Mean-Square (RMS) method

The associate editor coordinating the review of this manuscript and approving it for publication was Zhigang Liu.

is recommended in the standards [9], [10]. This method is nearly based on stationary assumptions and is widely used in many fields. Although using the RMS value to detect the voltage sag is simple and easy to implement in principle, it's prone to delay and susceptible to interference when extracting the characteristics of the voltage signal. For instance, in many cases when the voltage sag occurs, the RMS value of the voltage needs transition time to decrease to a specific value, and it will not decrease immediately. Similarly, the RMS value of the voltage will not be restored immediately after the fault is removed, which may cause errors in the detection of voltage sag. In addition, the standards also propose the use of Fast Fourier Transform (FFT). Still, due to the ambiguity of the voltage information in the transient when the voltage sag occurs and ends, FFT has shortcomings such as spectrum leakage and loss of time information.

The Wavelet Transform (WT) has been proposed in the literature [11], [12], which is also a commonly used method for signal analysis. WT analysis can provide uniform resolution for all signal scales, and it is the advantage that can make WT more efficient in processing signals with gradually changing frequencies. The most important step of WT is to determine the mother wavelet and the number of decomposition levels, but the choice is often subjective and difficult. Another shortage of the WT analysis is its non-adaptive feature. Discrete Wavelet Transform (DWT) and Maximum Overlap Discrete Wavelet Transform (MODWT) are also proposed for voltage disturbance detection [13], [14]. They can decompose the sampled signal into scale coefficients and wavelet coefficients, which can be analyzed to determine when the voltage sag starts and ends. Similarly, the crucial step of DWT or MDOWT is the choice of the mother wavelet, which affects the calculation of coefficients to a large extent [15], [16]. The Wigner-Ville distribution is also referred to as the Heisenberg wavelet and has been widely used in electrical engineering. The biggest disadvantage of this wavelet is that there will be severe cross-terms in some frequency ranges of the signal, which manifests as the existence of negative power [17].

In [18], [19], different detection methods are compared and analyzed in terms of detection accuracy and real-time performance, such as Kalman Filter (KF), FFT, DFT, and so on. The advantage of KF is that it can resist noise interference better. Still, its computational complexity will change with the influence of harmonics, and KF cannot track the fundamental voltage signal. Comparative analysis shows that almost all time-domain detection methods cannot completely overcome the interference of harmonics and noise, and they cannot give accurate results when the interference exists. At this time, an additional filter is needed to assist in extracting the fundamental voltage signal, but this will cause the phase delay of the voltage signal so that it cannot provide accurate phase jump information, which is an essential parameter for some devices. Besides, the results show that each method has a considerable time latency for detecting the voltage sag [20].

In recent years, the adaptive processing of signals has become popular research. Due to the characteristics of adaptive decomposition, extensive research has been conducted on the adaptive signal decomposition methods, including Empirical Mode Decomposition (EMD), Variational Mode Decomposition (VMD), etc. Among these methods, EMD is the earliest adaptive signal decomposition method proposed by Huang *et al.* [21] applied EMD to vibration signal analysis in gearbox fault location diagnosis, Liu *et al.* EMD is a multi-resolution, adaptive time-frequency domain analysis tool, which has been proved as an efficient tool for voltage signal decomposition and analysis in [22]–[25], during the frequency variations and in the presence of noise. It allows the voltage signal to be decomposed into a finite number of intrinsic modal functions (IMFs) and a residual trend. Two definitions are used to choose the IMFs: the number of extreme values and zero crossings must be equal or differ by at most one in the entire dataset; the average value of the envelope defined by the local maximum and the envelope defined by the local minimum is zero at any time. In addition, to overcome the problems of mode mixing in EMD, EMD has also been improved in recent years, such as the Ensemble Empirical Mode Decomposition (EEMD) [26]–[28], etc. EEMD improves the decomposition ability by adding Gaussian white noise and obtaining multiple averages. [29] combined EEMD with wavelet neural network to identify the faults of locomotive rolling bearings. But the voltage signal is not particularly complex; EEMD is too computationally expensive for voltage signal detection. On the other hand, Variational mode decomposition (VMD) is also an adaptive signal decomposition method, which can adaptively decompose a signal into several quasi-orthogonal bandwidth-limited intrinsic mode functions (BLIMFs). Each mode is tightly restricted within the frequency band near the center frequency in the spectral domain [30]. VMD method has shown a strong ability to solve the problems of mode mixing and misclassification. In some cases, VMD can extract signal features better than EMD and EEMD. Therefore, lots of studies have been conducted on VMD since it was put forward. In [31], the VMD was improved to extract weak bearing repetitive transient signals. VMD depends heavily on preset parameters, including mode number and bandwidth control parameters. Thus, choosing appropriate parameters to optimize the performance of VMD is crucial.

Adaptive decomposition can reflect the underlying oscillatory properties of the signals. Both EMD and VMD are commonly used in the analysis of voltage signals. Each signal can be decomposed into components with different frequencies by these two methods, and the instantaneous amplitude and instantaneous frequency of each component can be extracted using the Hilbert transform. The power frequency component can be extracted from them, which enables the detection and analysis of the signal. Therefore, we must choose a suitable method, which will be more efficient, depending on the spectrum of signals to be analyzed. However, EMD and VMD have not been applied to

real-time voltage signal detection due to their characteristics, which will be discussed later.

This paper focuses on the voltage detection problem for power quality management devices, such as DVR and UPS. The existing voltage detection algorithms are mainly based on the voltage root mean square value, the instantaneous voltage value, and the DQ transformation method of coordinates. However, these kinds of methods cannot overcome the voltage harmonic interference, which will delay the detection of the voltage. In order to overcome the interference of voltage harmonic and achieve rapid voltage sag detection, this paper proposes a tailored EMD-based adaptive real-time voltage signal expansion method for real-time voltage sag detection. Numerical simulations demonstrate that the proposed method has great performance in extracting voltage sag features under complex operational environments and can detect the voltage sag within 1 millisecond. The contributions are summarized as follows:

1) A tailored EMD-based adaptive real-time voltage signal detection method is proposed. As a result, the sampling voltage signal can be automatically expanded using the real-time voltage signal to achieve the rapid detection of voltage sag. To the best of our knowledge, this is the first application of EMD in the field of real-time voltage signal detection for power quality management devices.
2) Although some of the existing real-time voltage signal detection methods, such as RMS, can also detect voltage sag, they cannot overcome the interference of voltage harmonics well. The proposed tailored EMD-based adaptive real-time voltage signal detection method can overcome the endpoint effect and the interference of voltage harmonics, achieving great performance in extracting voltage sag features under complex operational environments.

The remainder of this paper is organized as follows. Section II briefly introduces the mathematical principles of EMD, VMD and Hilbert transform. Section III compares and analyzes the ability of EMD and VMD in decomposing voltage signals. Section IV proposes an improved EMD-based adaptive voltage signal expansion method for real-time voltage sag detection. Numerical results and conclusions are drawn in Sections V and VI.

II. PRINCIPLES OF MATHEMATICS

This section summarizes the basic mathematical principles of EMD, VMD, and Hilbert transform in voltage signal analysis.

A. EMPIRICAL MODE DECOMPOSITION (EMD)

The EMD can decompose any signal into a series of simple intrinsic modes of oscillations. Each oscillation mode is represented by an intrinsic mode function (IMF) with the following definitions [21]:

1) In the entire dataset, the number of extreme values and zero crossings must be equal or differ by at most one.
2) At any point, the average value of the envelope is defined by the local maximum, and the envelope defined by the local minimum is zero.

EMD can be done using the steps given below.

1. First, find the local maxima and local minima points of the analyzed signal $x(t)$ and mark them.

2. Then connect all the local maxima by a cubic spline to obtain the envelope of the maxima curve $p_{\max}(t)$. Repeat the procedure for the local minima to produce the lower envelope $p_{\min}(t)$.

3. Compute the mean of the envelopes $m(t)$.

$$m(t) = \frac{p_{\max}(t) + p_{\min}(t)}{2} \tag{1}$$

4. Extract the first potential IMF (Proto-mode function) $c_1(t)$.

$$c_1(t) = x(t) - m(t) \tag{2}$$

5. Whether $c_1(t)$ satisfy the definitions of IMF. And if $c_1(t)$ doesn't satisfy the definitions, then replace $x(t)$ with $c_1(t)$ and repeat steps 1 to 4 until the calculated $c_1(t)$ meets the definitions. Determine $c_1(t)$ as IMF-1.

6. Separate $c_1(t)$ from $x(t)$ to obtain the residue $r_1(t)$.

$$r_1(t) = x(t) - c_1(t) \tag{3}$$

The sifting process of EMD can be stopped when the residue $r_1(t)$ becomes a monotonic function from which no more IMFs can be extracted. If not, $r_1(t)$ is treated as the new data and subjected to the same sifting process described above to obtain a new IMF and a new residue.

After signal decomposition, the original signal $x(t)$ can be reconstructed as:

$$x(t) = \sum_{i=1}^{n} c_i(t) + r_n(t) \tag{4}$$

After that, we can process these components separately.

B. VARIATIONAL MODE DECOMPOSITION (VMD)

The VMD can adaptively decompose the original signal $x(t)$ into a series of modes $b_k(t)$, each mode $b_k(t)$ vibrates closely around a center frequency f_k [30].

VMD is the search for the optimal solution of the following constrained variational modes. Specifically, the decomposition process of VMD is to solve the constrained variational problem and the constrained variational problem of signal $x(t)$ is:

$$\min_{\{b_k\},\{f_k\}} \left\{ \sum_k \left\| \partial_t \left[\left(\delta(t) + \frac{j}{\pi t} \right) \times b_k(t) \right] e^{-jf_k t} \right\|_2^2 \right\} \tag{5}$$

$$\sum_k b_k = x(t) \tag{6}$$

among them, $\{b_k\} = \{b_1, b_2, \cdots, b_K\}$ represents the set of K modal components in total, and $\{f_k\}$ is the set of corresponding center frequencies for each mode, $\delta(t)$ is Dirac distribution.

By introducing the augmented Lagrangian $\mathcal{L}$, the constrained variational problem above can be transformed as follows:

$$\begin{aligned} &L\left(\{b_k\},\{f_k\},\lambda\right) \\ &\quad=\alpha\sum_k\left\|\partial_t\left[\left(\delta(t)+\frac{j}{\pi t}\right)\times b_k(t)\right]e^{-jf_kt}\right\|_2^2 \\ &\qquad+\left\|x(t)-\sum_k b_k(t)\right\|_2^2 \\ &\qquad+\langle\lambda(t),x(t)-\sum-kb_k(t)\rangle \end{aligned} \tag{7}$$

where λ is Dual ascent and α is the Lagrange multiplier.

The process of updating b_k and f_k from equation (7) is summarized as follows:

1. $\left\{\hat{b}_k^1\right\}$ and $\left\{\hat{f}_k^1\right\}$, $\hat{\lambda}^1$ are initialized.
2. Dual ascent λ should update for all $f \geq 0$.

$$\hat{\lambda}^{n+1}(f)=\hat{\lambda}^n(f)+\tau\left(\hat{x}(f)-\sum_k\hat{b}_k^{n+1}(f)\right) \tag{8}$$

3. Next, each mode needs to be updated iteratively in turn for all $f \geq 0$.

$$\hat{b}_k^{n+1}(f)=\frac{\hat{x}(f)-\sum_{i<k}\hat{b}_i^{n+1}(f)-\sum_{i>k}\hat{b}_i^n(f)+\frac{\hat{\lambda}^n(f)}{2}}{1+2\alpha\left(f-f_k^n\right)^2} \tag{9}$$

where n represents the number of iterations.

4. At the same time, the update of frequency can be expressed as:

$$f_k^{n+1}=\frac{\int_0^\infty f\left|\hat{b}_k^{n+1}(f)\right|^2df}{\int_0^\infty\left|\hat{b}_k^{n+1}(f)\right|^2df} \tag{10}$$

The stoppage criterion of the iterative update:

$$\sum_k\left\|\hat{b}_k^{n+1}-\hat{b}_k^n\right\|_2^2/\left\|\hat{b}_k^n\right\|_2^2<\epsilon \tag{11}$$

Through the decomposition above, the signal $x(t)$ is decomposed into a series of modes b_k around the corresponding center frequency f_k.

C. HILBERT TRANSFORM (HT)

The complex conjugate $y(t)$ of any real-valued function $c(t)$ can be determined through Hilbert Transform [32].

For arbitrary time series $c(t)$, the corresponding Hilbert transform $h(t)$ is as follows:

$$h(t)=\frac{1}{\pi}\mathrm{PV}\int_{-\infty}^{+\infty}\frac{c(\tau)}{t-\tau}d\tau \tag{12}$$

where the PV indicates the principal value of the singular integral. With the Hilbert transform $h(t)$, the analytic signal $y(t)$ can be expressed as:

$$y(t)=c(t)+jh(t)=A(t)e^{j\theta(t)} \tag{13}$$

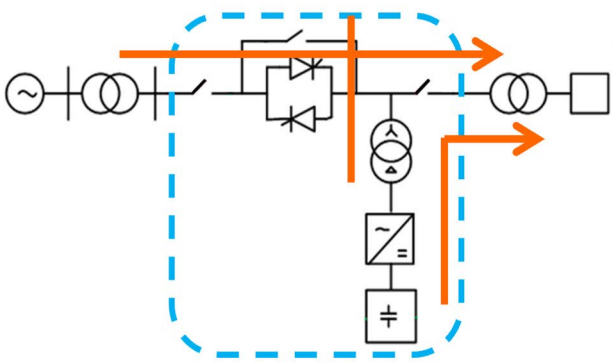

FIGURE 1. Topology of parallel switched DVR.

Here, $A(t)$ represents the instantaneous amplitude and $\theta(t)$ represents instantaneous phase angle.

Through the summarization above, EMD and VMD can decompose the input signal into various oscillation modes with different amplitude and frequencies. We can use Hilbert Transform for each mode to obtain the corresponding analytic signal and extract the essential information. One of the differences between EMD and VMD is that VMD can specify the number of modes to be decomposed, while EMD cannot. However, any differences or connections between these modes will be studied and compared in the next section through the analysis of voltage signals by both EMD and VMD methods.

D. DYNAMIC VOLTAGE REGULATOR (DVR)

The DVR is mainly composed of inverters, output transformers, static switches, and energy storage devices. The figure below shows the topology of the parallel switching DVR we studied. Parallel switching DVR is a new voltage restorer that is currently the most advanced, with stronger adaptability. Under normal circumstances, it works in the thyristor conduction mode and directly supplies power to the load from the power grid. When there is a short-term voltage change, it switches to the inverter to supply power. If the energy storage device chooses the supercapacitor system, it can provide a second-level backup. And if the battery system is used, it can manage long-term interruptions.

In order to achieve voltage sag control, it is necessary to achieve fast voltage signal detection. The equipment we have developed can quickly analyze and process voltage signals for detection.

III. COMPARATIVE ANALYSIS OF EMD AND VMD IN VOLTAGE SAG DETECTION

Although the EMD and VMD have been proposed and applied to voltage signal analysis, their similarities and differences in analyzing voltage signals have not been thoroughly investigated. In order to better apply adaptive processing technology in real-time voltage sag detection, this

TABLE 1. Voltage signal parameters.

A_1	A_3	A_5	A_7	f_1	f_3	f_5	f_7
1.0	0.05	0.1	0.08	50Hz	150Hz	250Hz	350Hz

section compares and analyzes the performance of EMD and VMD in decomposing voltage signals and voltage sag signals.

Firstly, we will test the performance of EMD and VMD that depends on decomposing the different types of voltage signals into intrinsic modes and compare the results. In [23] and [33], high-amplitude harmonics are added to the voltage signal on voltage signal detection, which is relatively easy to analyze. In addition, through communication with equipment manufacturers, the difficulty in voltage sag detection for DVR and UPS mainly lies in the interference of the 3rd, 5th, and 7th voltage harmonics [4], [5]; and only the voltage harmonics below the seventh order will be considered in this paper. Therefore, the relevant parameters of the tested voltage signal are set as follows.

$$u(t) = \sum_{i=0}^{3} A_{2i+1} \times \sin(2\pi t f_{2i+1}) \tag{14}$$

where,

A_1 is the amplitude of the fundamental voltage.
A_3 is the amplitude of the third harmonic voltage.
A_5 is the amplitude of the fifth harmonic voltage.
A_7 is the amplitude of the seventh harmonic voltage.
f_1 is the frequency of the fundamental voltage.
f_3 is the frequency of the third harmonic voltage.
f_5 is the frequency of the fifth harmonic voltage.
f_7 is the frequency of the seventh harmonic voltage.

Using the standardized value for the amplitude to facilitate the analysis. The parameters are set as shown in the table below.

As shown in Figure2, the voltage signal of the fundamental frequency is 50 Hz, with a sampling frequency of 10 kHz and a time window of 0.41 seconds. In order to show the details of the voltage waveform better, only the 100 milliseconds of the waveform are captured in the figure below.

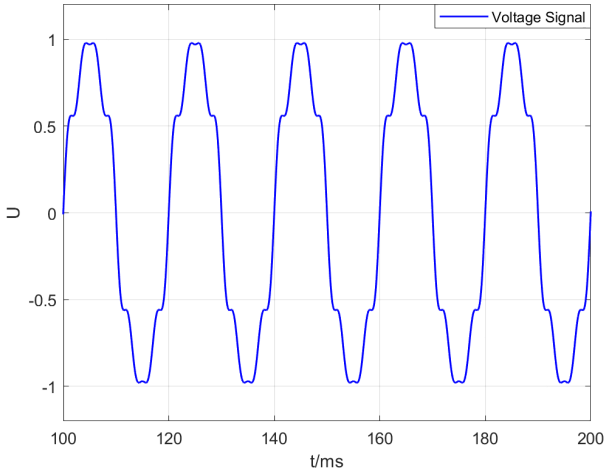

FIGURE 2. Voltage signal.

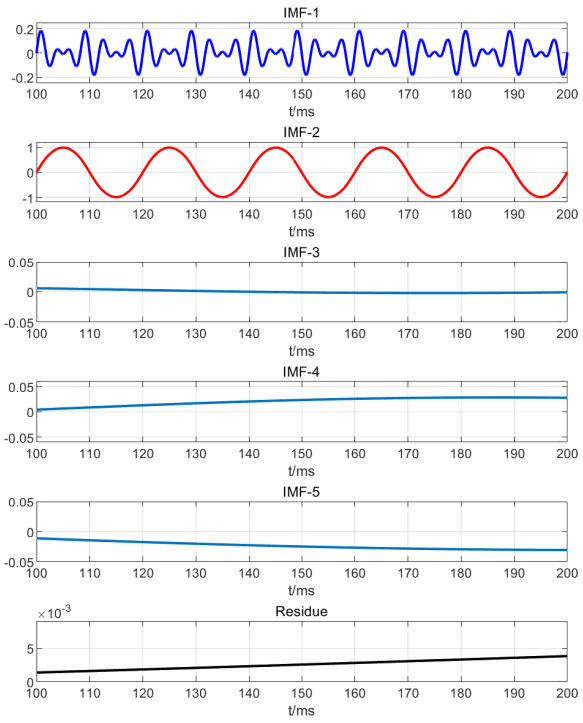

FIGURE 3. Decomposition of the voltage signal by EMD.

A. THE DECOMPOSITION OF THE VOLTAGE SIGNAL

Figure 3 and Figure 4 show the results that the voltage signal has been decomposed by EMD and VMD, and the number of modes for VMD is set to 5. As shown in the Figures, both these two methods can decompose the voltage signal from high to low frequency.

As shown in Figure 3, the number of IMFs decomposed from the voltage signal by EMD is also 5. It could be seen from Figure 4 that IMFs decomposed by VMD nearly contain the fundamental voltage (IMF-5) and all harmonic components (IMF-2 to IMF-4). But for EMD, only the fundamental voltage (IMF-2) is decomposed from the original signal, it could be found that the IMF-1 in Figure 3 shows the total harmonic components if we observe carefully. Hence the VMD method is more suitable to extract high-frequency harmonic components from the voltage signal than EMD.

However, all these modes decomposed by two methods contain meaningless components such as IMF-3, IMF-4, IMF-5 in Figure 3, and IMF-1 in Figure 4, which are caused by endpoints.

Apart from this, the distortion at the endpoints of VMD is more severe than EMD seen from the decomposed meaningful voltage waveform in Figures 5 and 6.

The instantaneous frequency of each mode can be visualized from the Hilbert transform, as shown in Figure 7 and Figure 8. It can be seen that the frequency of mode IMF-2 decomposed by EMD is 50 Hz, and the frequencies of modes IMF-2 to IMF-5 decomposed by VMD are 350Hz, 250 Hz,

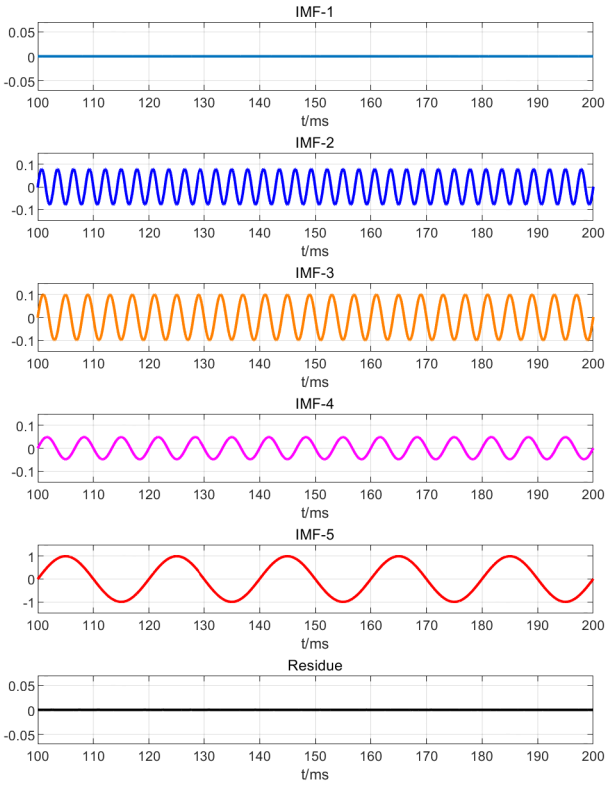

FIGURE 4. Decomposition of the voltage signal by VMD.

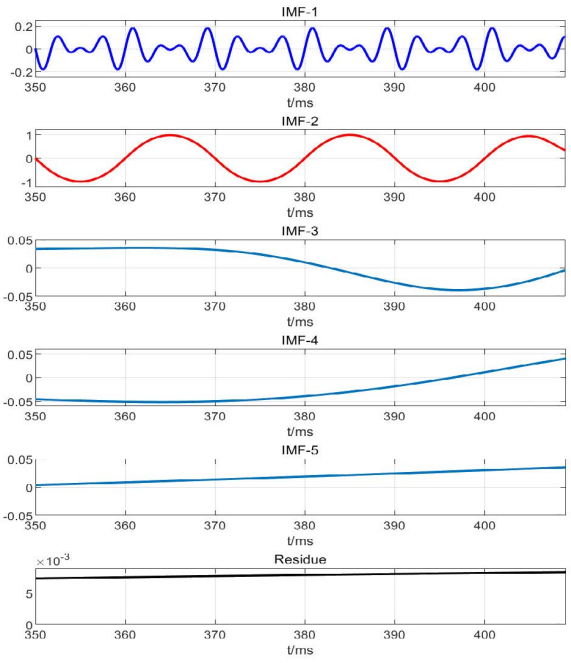

FIGURE 5. Endpoints of decomposition by EMD.

and 150 Hz, respectively. The results of decomposition above are also confirmed in the Figures.

When the harmonic voltage has a high amplitude, it could also be accessible for EMD to decompose the voltage signal to extract information about the fundamental voltage and the

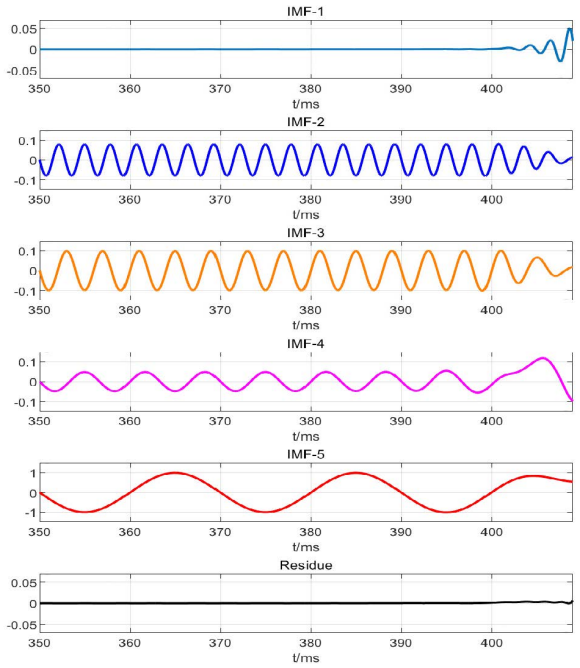

FIGURE 6. Endpoints of decomposition by VMD.

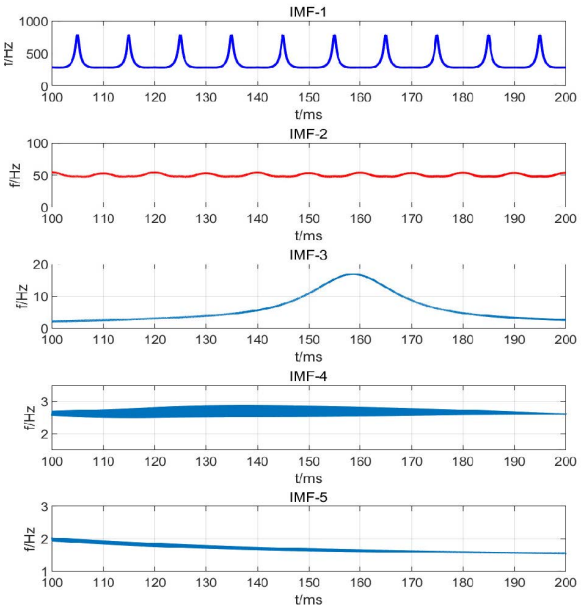

FIGURE 7. The frequency of IMFs (EMD).

high-frequency harmonic voltage. By comparison, the ability to extract signals of VMD is better than EMD.

B. THE DECOMPOSITION OF THE VOLTAGE SAG SIGNAL

EMD and VMD have been shown to be able to decompose the normal voltage signal into a series of modes. The decomposition of the voltage sag signal could be tested in this part. Most previous analyses of voltage sag have been targeted at a deep and prolonged sag [24], which is the easiest to be detected. Therefore, the depth of voltage sag is set to 25%, and the duration of sag is set to 34ms to check the

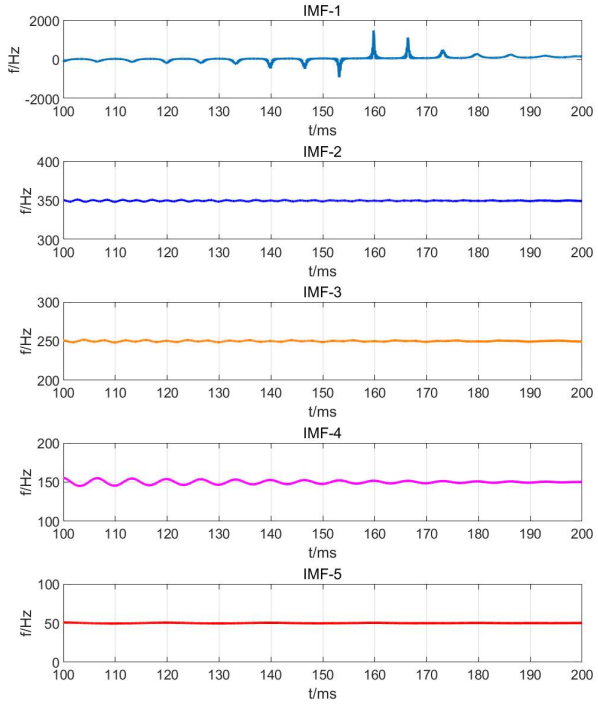

FIGURE 8. The frequency of IMFs (VMD).

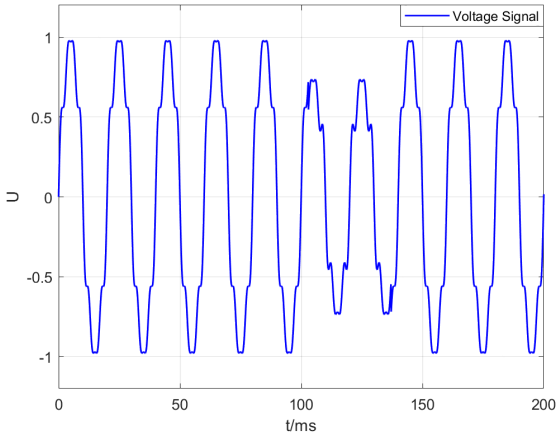

FIGURE 9. Voltage sag signal.

performance of these two methods better. Also, the depth of the voltage sag uses the standardized value.

Firstly, considering the voltage sag occurs at the fundamental voltage.

$$\text{sag}_1 = 0.25\sin(2\pi f_1 t) \tag{15}$$

And the time interval of sag is 0.103 seconds to 0.137 seconds and the voltage signal u_{s1} can be described as:

$$u_{s1}(t) = u(t) - \text{sag}_1 \times (t \geq 0.103 \& t \leq 0.137) \tag{16}$$

Figure 9 shows the voltage sag signal.

Using EMD and VMD to decompose the voltage sag signal u_{s1}. The decomposition results have been shown in Figure 10 and Figure 11.

It can be seen from Figure 10 that the voltage sag signal is decomposed into 6 IMFs by EMD, which are one

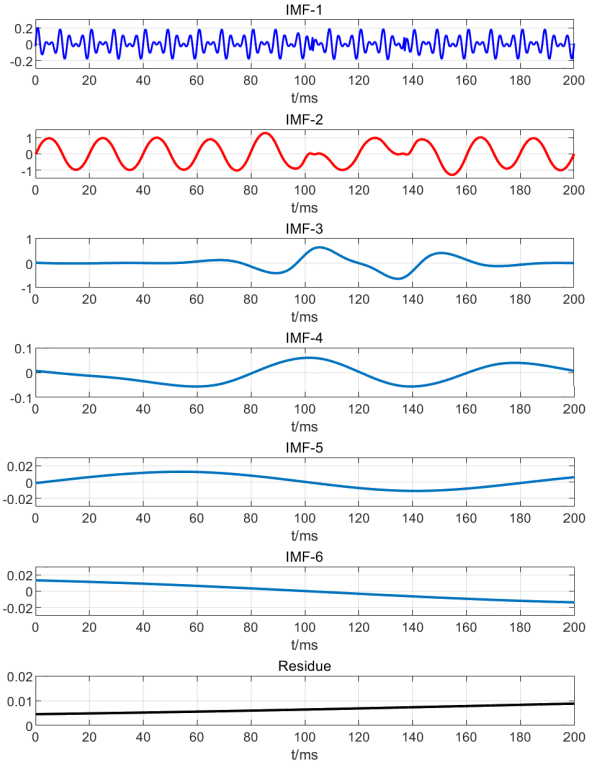

FIGURE 10. Decomposition of the voltage sag signal by EMD.

more than normal, due to the occurrence of voltage sag so that the extreme point configuration changes. Obviously, the fundamental voltage (IMF-2) has experienced a sudden change, and the amplitude of IMF-2 has been significantly reduced. And IMF-1 has been a slight fluctuation in Figure 10. The sudden change of the fundamental voltage will make it easier to detect voltage sag quickly.

The number of IMFs decomposed by VMD is still 5 in Figure 11. Besides, only the fundamental voltage (IMF-5) has experienced a slight and smooth transition, and other IMFs have been obvious mutations in Figure 11. Except for the component IMF-1, which is meaningless, the seventh harmonic voltage (IMF-2) has an abrupt drop when the sag occurs and ends. The third harmonic voltage (IMF-4) is just the opposite; it rises suddenly at the same moment. Although the fluctuation of the fifth harmonic voltage (IMF-3) is more subdued than IMF-2 and IMF-4, it is still more obvious than the fluctuation of IMF-5. In other words, the sag on the fundamental voltage will impact the high-frequency harmonics. However, the slight and smooth transition process of the fundamental voltage (IMF-5) may lead to errors and delays in detection.

From the analysis of this section above, both EMD and VMD can decompose signals and extract the fundamental voltage, which is essential information for analysis. The biggest difference in decomposition between EMD and VMD is the harmonic signals. VMD can completely separate all high-frequency harmonic components from the original signal, even high-frequency harmonic components with a

low amplitude. These components would experience obvious fluctuations when a voltage sag occurs in the fundamental voltage, which means VMD is sensitive to high-frequency harmonic components. But EMD cannot extract high-frequency harmonic components of low amplitude from the signal and only shows the sum of harmonics.

Another important point to pay attention to is that the modes decomposed by VMD have severe distortion at the endpoints of the signal, which is extremely easy to cause misjudgment of voltage detection. In contrast, the modes decomposed by EMD with lesser distortion, although there are endpoint effects. In fact, through repeated experiments, it has been found that voltage signals with integer multiples are usually more conducive to decomposition for EMD, and the decomposed modes hardly contain meaningless components.

IV. TAILORED EMD-BASED ADAPTIVE REAL-TIME VOLTAGE SIGNAL EXPANSION METHOD

In the past, EMD and VMD analysis have been used to monitor the entire signal and have not been applied in the field of real-time detection. As can be seen from the analysis in the previous part, the biggest limitation is that both VMD and EMD are largely dependent on the signal length. Especially for EMD, the decomposition result largely depends on the selection of extreme points. In real-time detection, it is necessary to determine the fault as quickly as possible after the fault occurs. We can only obtain a signal of 1 to 2 milliseconds or even shorter after the fault occurs. In addition, EMD has severe end effects, which could result in distortion of the extracted signal near the start and end after the original signal is decomposed. Suppose such a short fault signal is decomposed by using EMD. In that case, it is easy to fail to decompose the fault signal or to make a false diagnosis, even if more information about the original signal before the fault is stored. These are important reasons that limit the application of these two methods in real-time detection.

The analysis of these two methods in the previous section shows that the distortion of the modes decomposed by VMD at the endpoints of the voltage signal is more severe than EMD. Therefore, an EMD-based adaptive real-time voltage signal expansion method for real-time voltage sag detection is described in this section. The difficulty of applying EMD to real-time detection lies in whether it can use limited signal data to decompose fault characteristic components in time when voltage sag occurs and must overcome endpoint effects.

It can be seen from the analysis above, for EMD, each IMF requires multiple ''screening'' processes, and for each screening process, the local average value of the signal needs to be calculated based on the upper and lower envelopes. The upper (lower) envelope is obtained from the local maximum (small) value of the signal through 3rd order spline interpolation. Due to the number of extreme points near the endpoints of the signal being limited, and the voltage signal cannot be at the maximum or minimum value at the endpoint at the same time, the upper and lower envelopes will diverge at both ends of the data sequence, which results in the information at the endpoints of the signal being unavailable although the fundamental frequency voltage signal can be decomposed by EMD. Therefore, when the length of the characteristic sequence of the voltage signal at the end is insufficient, EMD cannot accurately decompose the corresponding characteristic waveform. The extreme point continuation method is often used to solve this problem, but it also can easily cause the abnormal decomposition of EMD; that is, the fault waveform is incorrectly decomposed. Based on this, we can consider adding a sequence of waveforms at the end of the voltage signal to make up for the shortcomings of insufficient information at the end and extract the corresponding characteristics of the end of the voltage signal. And because of the periodic characteristics of the voltage signal, we can use the waveform information of the previous cycle to supplement the end of the real-time sampling signal, which can ensure the authenticity of the voltage signal to the greatest extent.

Based on the analysis above, this paper proposes a tailored EMD-based adaptive real-time voltage signal expansion method for real-time voltage sag detection.

Insufficient signal length is the main cause of incomplete decomposition; this paper proposes a method of automatic expansion of voltage signals with the following steps:

Step 1: In sampling, about 1 cycle of voltage waveform information P is stored in real-time;

Step 2: Obtain the amplitude A_1 of voltage at the endpoint a of the real-time sampling waveform;

Step 3: Determine the point b where the voltage amplitude A_1 is obtained for the first time in the real-time stored waveform;

Step 4: Obtain the current time series value $t(x)$ at point b, and determine the point c at the time series value $t(x+1)$;

Step 5: Intercept about the half-cycle waveform Q starting from point c;

Step 6: The complete waveform W is obtained after supplementing the waveform Q to point a.

Figure 12 is the explanatory diagram of the real-time voltage signal expansion method. Figure 13 is the flow chart of the method proposed in this paper.

We note that the configuration of the extreme points of the expanded voltage signal will change when voltage sag occurs. The detection and identification of voltage sag can be quickly achieved by using this change.

Through expanding the voltage signal above, we can briefly describe the voltage sag detection method proposed in this paper as shown in the following block diagram.

As shown in Figure 14, the module M represents real-time sampling and stores voltage signals about 1 cycle.

The module N represents that the voltage signal in module M is expanded by the above-mentioned voltage signal expansion method.

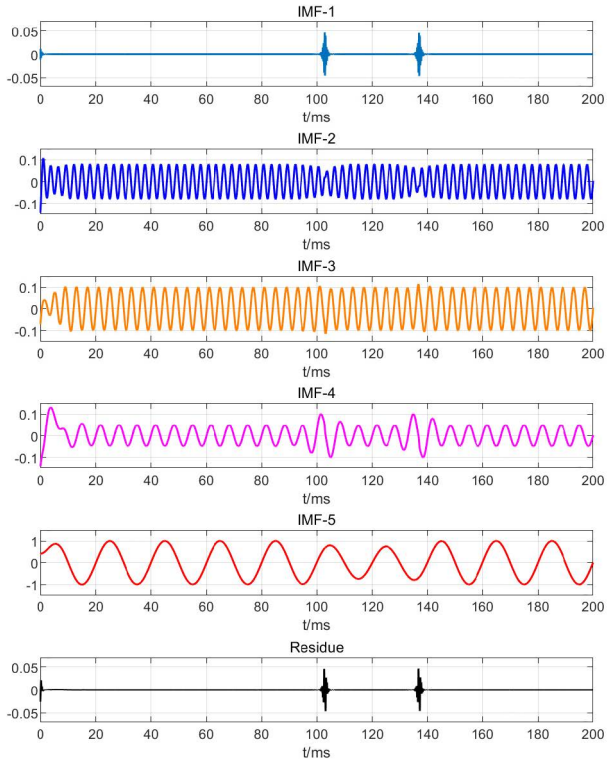

FIGURE 11. Decomposition of the voltage sag signal by VMD.

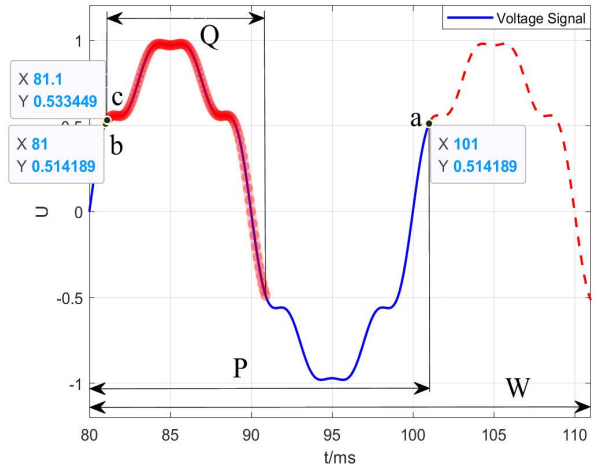

FIGURE 12. Signal Expansion Illustration.

The module X represents that the voltage signal processed by module N is decomposed by using EMD.

The judging module Z represents whether the fundamental voltage component decomposed in module X is within the set threshold range. If the fundamental component is within the threshold range, it returns to module M; and if the fundamental component deviates from the threshold range, it's determined that voltage sag occurs.

As shown in the block diagram, it is judged whether voltage sag occurs through the result output by module Z. After that, the detection flow is repeated.

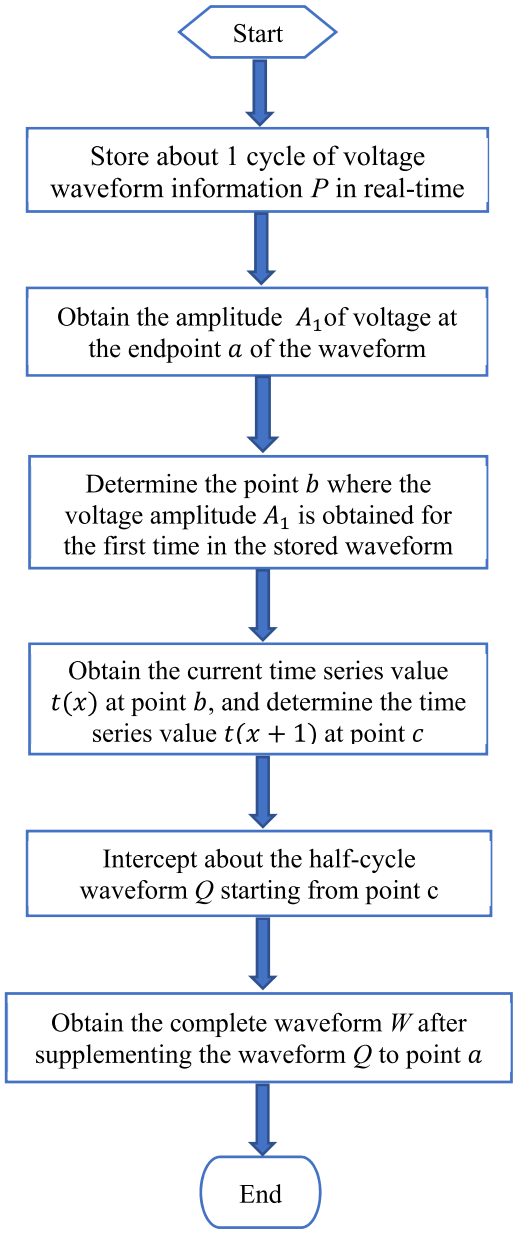

FIGURE 13. Flowchart of the adaptive real-time voltage signal expansion method.

V. NUMERICAL RESULTS

A. THE DECOMPOSITION OF THE SHORT-TERM VOLTAGE SIGNAL

First of all, the performance of EMD in decomposing the voltage signal with a shorter length could be tested. Intercepting a section of the voltage signal for decomposition, and the voltage signal is described as:

$$u_2(t) = u(t) \times (t \geq 0.08 \& t \leq 0.111) \tag{17}$$

It can be shown in Figure 15.

Then this short-term voltage signal is decomposed using EMD, which is shown in Figure 16. The dotted line in the figure is the set threshold interval. The threshold interval is set as follows.

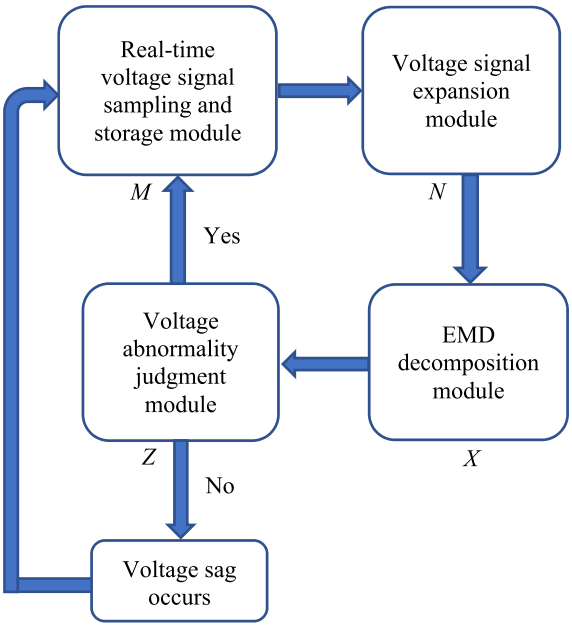

FIGURE 14. Block of the voltage sag detection based on voltage signal expansion and EMD.

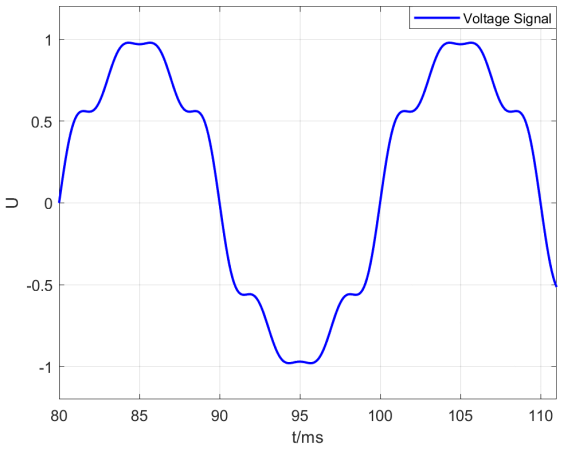

FIGURE 15. Short-term voltage signal.

The upper threshold is:

$$u_{\mathrm{UL}} = A_1 \sin(2\pi f_1 t) + 15\% \tag{18}$$

The lower threshold is:

$$u_{\mathrm{LL}} = A_1 \sin(2\pi f_1 t) - 15\% \tag{19}$$

As shown in Figure 16, the number of IMFs decomposed by the EMD for the short-term voltage signal is two. EMD can still be used to accurately extract the fundamental voltage component (IMF-2) and total harmonic component (IMF-1). And IMF-2 is within the set threshold range. The result of decomposition also shows that the method proposed in this paper doesn't produce wrong judgment results under normal circumstances.

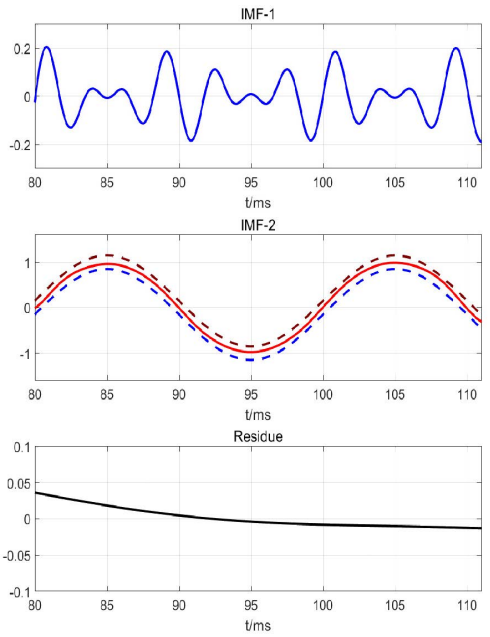

FIGURE 16. Decomposition of the short-term voltage signal by EMD.

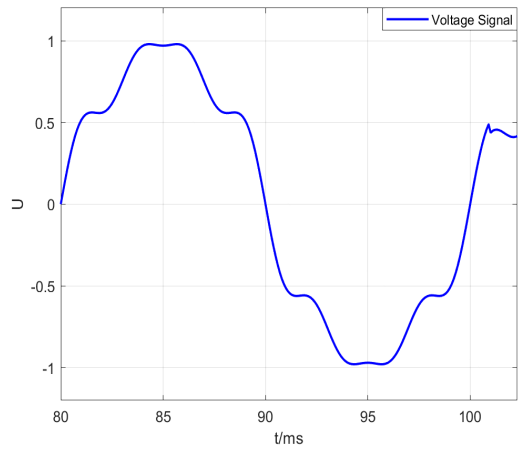

FIGURE 17. Real-time voltage sag signal.

B. THE DECOMPOSITION OF REAL-TIME VOLTAGE SAG SIGNAL

Next, the EMD is used to decompose the real-time voltage sag signal. Considering the endpoint effect, we intercept the waveform information about 2 milliseconds after the occurrence of the voltage sag and retain the waveform information about 1 cycle before the occurrence of the voltage sag. Similarly, considering the voltage sag occurs at the fundamental voltage.

$$\mathrm{sag}_2 = 0.25 \sin(2\pi f_1 t) \tag{20}$$

The voltage sag signal is expressed as follows:

$$u_{s2}(t) = \left(u(t) - \mathrm{sag}_2 \times (t \geq 0.101 \& t \leq 0.137)\right) \times (t \geq 0.008 \& t \leq 0.1029) \tag{21}$$

Figure 17 shows the signal.

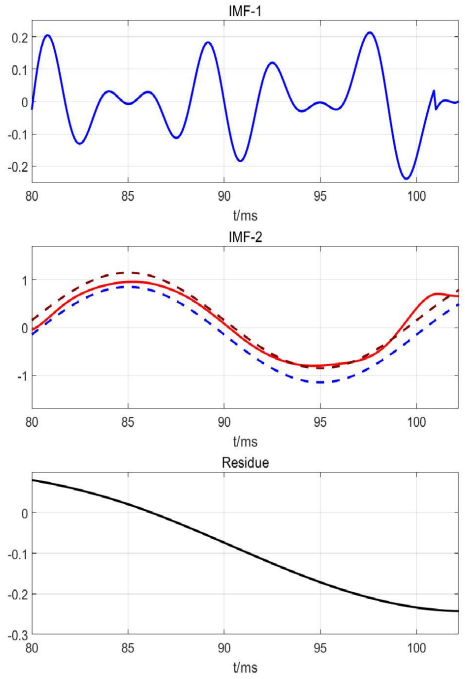

FIGURE 18. Decomposition of the real-time voltage sag signal by EMD.

EMD is used to decompose the real-time voltage sag signal, and the results of decomposition are shown in Figure 18. The dotted line in the figure is the set threshold interval. The threshold is the same as that described in equations (18) and (19).

As shown in Figure 18, the fundamental voltage component (IMF-2) and the total harmonic component (IMF-1) fluctuate slightly. Although EMD can decompose the fault waveform when voltage sag occurs, the result is unclear. The fundamental voltage component coincides with the threshold limit, easily leading to detection delay or even misjudgment. After repeated tests, EMD needs at least 5 milliseconds of waveform information after the sag to be able to more accurately decompose the fault waveform, which is undoubtedly an excessively long time for some precision instruments.

C. TAILORED EMD-BASED ADAPTIVE REAL-TIME VOLTAGE SIGNAL EXPANSION

The real-time voltage signal expansion method proposed in this paper is applied to voltage sag detection. In order to test the performance of the method, we intercept the waveform information of 0.9 milliseconds after the occurrence of the voltage sag and retain the waveform information of about 1 cycle before the occurrence of the voltage sag. Also, considering the voltage sag occurs at the fundamental voltage.

The new real-time voltage sag signal above can be re-described as follows.

$$u_{s3}(t) = \left(u(t) - \text{sag}_2 \times (t \geq 0.101 \& t \leq 0.137)\right) \times (t \geq 0.008 \& t \leq 0.1019) \quad (22)$$

The new real-time voltage sag signal is shown in Figure 19.

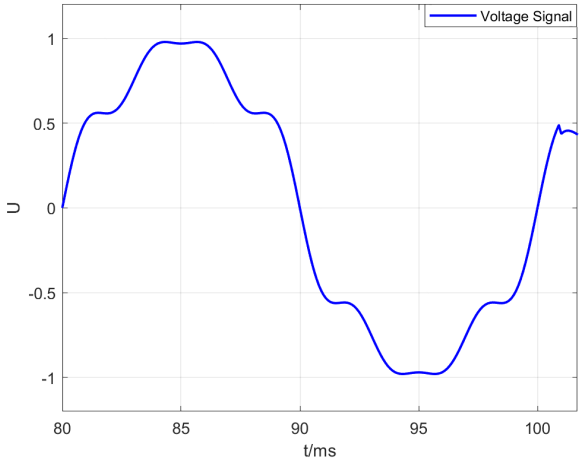

FIGURE 19. Real-time voltage sag signal.

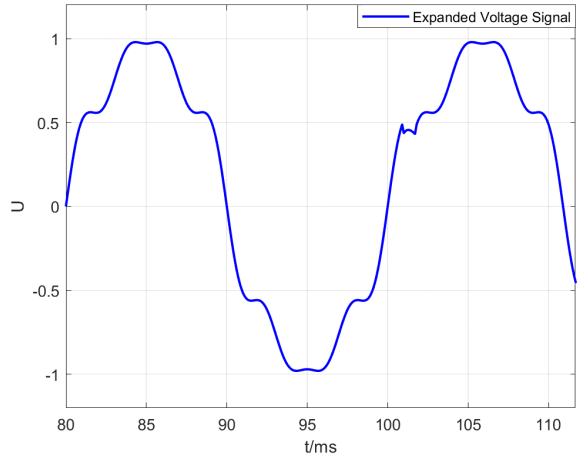

FIGURE 20. Expanded voltage sag signal.

Waveform expansion is performed on the new real-time voltage sag signal, and then EMD is performed on the expanded voltage sag signal. The expanded signal is shown in Figure 20, and the results of decomposition are shown in Figure 21. The dotted line in the figure is the set threshold interval. The threshold is the same as that described in equations (18) and (19).

As shown in Figure 20, the configuration of extreme points of the expanded voltage sag signal changes when voltage sag occurs. From the results of decomposition, it can be clearly seen that the fault waveform (IMF-2) is accurately decomposed from the expanded voltage sag signal by EMD. The fundamental voltage component IMF-2 has changed drastically, deviating from setting the threshold interval. Only the waveform information of 0.9 milliseconds after the voltage sag is required. This also means that our method can detect the voltage sag within 1 millisecond after it occurs. It has been greatly improved compared with the previous waveform information that requires at least 5 milliseconds after the occurrence of the voltage sag.

From the analysis in this section above, the ability of EMD to decompose the short-term voltage signal has been tested.

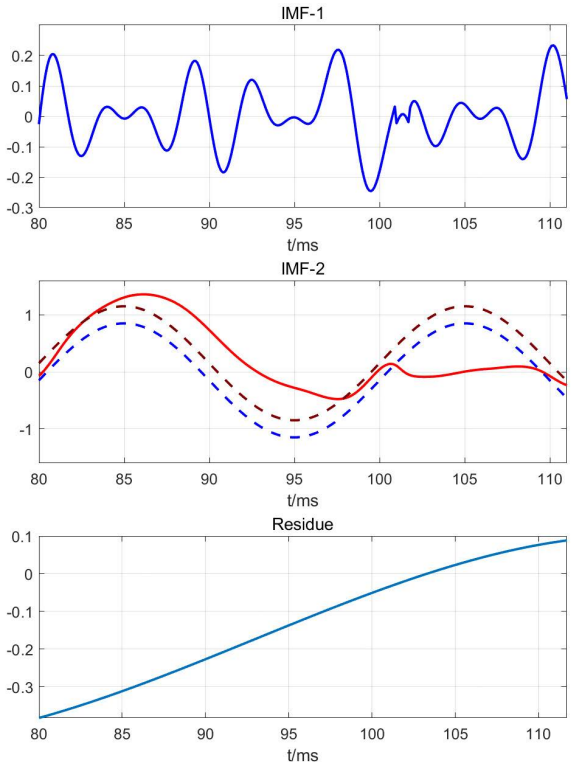

FIGURE 21. Decomposition of expanded voltage sag signal by EMD.

EMD can completely decompose the real-time voltage signal and has good performance under normal conditions; however, when voltage sag occurs, it cannot accurately decompose the fault component from the voltage signal due to the endpoint effect. Using the real-time voltage signal expansion can effectively overcome the endpoint effect, and combining it with EMD can decompose the fault components within 1 millisecond. The analysis results show that the method can overcome harmonic interference to achieve tracking of the fundamental voltage signal and achieve ultra-fast voltage sag detection.

VI. CONCLUSION

In this paper, the actual performances of EMD and VMD in real-time voltage signal detection are compared and analyzed, where both of them can accurately decompose the voltage signals. VMD has a greater advantage in decomposing high-frequency components than EMD. However, VMD is more sensitive to high-frequency components than EMD when a voltage sag occurs. Instead, EMD can extract the information of the fundamental frequency component better. When a voltage sag occurs, EMD can decompose the fault information accurately. Besides, the distortion of IMFs decomposed by VMD at the endpoints of the voltage signal is more severe than EMD. For short-term voltage signals, although EMD can still decompose these voltage signals effectively, it cannot identify faults accurately in a short time due to the endpoint effect.

In order to overcome the drawbacks of these two methods in real-time voltage sag detection, this paper proposes a tailored EMD-based adaptive voltage signal expansion method for real-time voltage sag detection, which can effectively avoid harmonic interference and overcome the endpoint effect of traditional EMD. In the proposed tailored EMD method, the sampling voltage signal is automatically expanded using the real-time voltage signal, which can achieve the rapid detection of voltage sag under complex operational environments. Numerical results demonstrate that the proposed method can detect the voltage sag within 1 millisecond.

REFERENCES

[1] S. Hasan, N. Gurung, K. M. Muttaqi, and S. Kamalasadan, "Electromagnetic field-based control of distributed generator units to mitigate motor starting voltage dips in power grids," *IEEE Trans. Appl. Supercond.*, vol. 29, no. 2, pp. 1–4, Mar. 2019.

[2] J. P. González, A. M. S. M. San Roque, and E. A. Perez, "Forecasting functional time series with a new Hilbertian ARMAX model: Application to electricity price forecasting," *IEEE Trans. Power Syst.*, vol. 33, no. 1, pp. 545–556, Jan. 2017.

[3] A. Espin-Delgado, J. R. Camarillo-Peñaranda, and G. Ramos, "Characterization of phase-angle jump in radial systems using incremental voltage phasors," *IEEE Trans. Ind. Appl.*, vol. 55, no. 2, pp. 1117–1125, Mar./Apr. 2018.

[4] H. Sha *et al.*, "An accurate detection algorithm for voltage sag homologous data based on key point matching of trajectory features," *Automat. Electr. Power Syst.*, no. 6, pp. 109–116, 2022.

[5] A. Hu *et al.*, "Overview of voltage sag control measures and equipment," *Power Electron. Technol.*, vol. 53, no. 7, pp. 1–5&10, 2019.

[6] M. J. Afroni, D. Sutanto, and D. Stirling, "Analysis of nonstationary power-quality waveforms using iterative Hilbert Huang transform and SAX algorithm," *IEEE Trans. Power Del.*, vol. 28, no. 4, pp. 2134–2144, Oct. 2013.

[7] Y. Wang, M. H. Bollen, and X. Y. Xiao, "Calculation of the phase-angle-jump for voltage dips in three-phase systems," *IEEE Trans. Power Del.*, vol. 30, no. 1, pp. 480–487, Feb. 2014.

[8] M. M. Rahman and M. N. Uddin, "Online unbalanced rotor fault detection of an IM drive based on both time and frequency domain analyses," *IEEE Trans. Ind. Appl.*, vol. 53, no. 4, pp. 4087–4096, Jul./Aug. 2017.

[9] *IEEE Guide for Voltage Sag Indices*, IEEE Standard 1564-2014, 2014.

[10] *Electromagnetic Compatibility (EMC)-Part 4-30: Testing and Measurement Techniques-Power Quality Measurement Methods*, IEC Standard 61000-4-30, ed. 3.0, 2015.

[11] S. Hasan, K. M. Muttaqi, and S. Kamalasadan, "An Approach to minimize the motor starting voltage dip using voltage support DG controller," in *Proc. IEEE Int. Conf. Appl. Supercond. Electromagn. Devices (ASEMD)* Apr. 2018, pp. 1–2.

[12] M. B. Latran and A. Teke, "A novel wavelet transform based voltage sag/swell detection algorithm," *Int. J. Electr. Power Energy Syst.*, vol. 71, pp. 131–139, Oct. 2015.

[13] S. Li and X. Wang, "Cooperative change detection for voltage quality monitoring in smart grids," *IEEE Trans. Inf. Forensics Security*, vol. 11, no. 1, pp. 86–99, Jan. 2015.

[14] J. Peng, "Assessment of transformer energisation transients and their impacts on power systems," Ph.D. dissertation, Univ. Manchester, Manchester, PL, U.K., 2013.

[15] Y. Wang, A. Bagheri, M. H. Bollen, and X. Y. Xiao, "Single-event characteristics for voltage dips in three-phase systems," *IEEE Trans. Power Del.*, vol. 32, no. 2, pp. 832–840, Apr. 2016.

[16] F. B. Costa and J. Driesen, "Assessment of voltage sag indices based on scaling and wavelet coefficient energy analysis," *IEEE Trans. Power Del.*, vol. 28, no. 1, pp. 336–346, Jan. 2012.

[17] S. Santoso, E. J. Powers, W. M. Grady, and P. Hofmann, "Power quality assessment via wavelet transform analysis," *IEEE Trans. Power Del.*, vol. 11, no. 2, pp. 924–930, Apr. 1996.

[18] Y. Xi, Z. Li, X. Zeng, X. Tang, Q. Liu, and H. Xiao, "Detection of power quality disturbances using an adaptive process noise covariance Kalman filter," *Digit. Signal Process.*, vol. 76, pp. 34–49, May 2018.
[19] A. Moschitta, P. Carbone, and C. Muscas, "Performance comparison of advanced techniques for voltage dip detection," *IEEE Trans. Instrum. Meas.*, vol. 61, no. 5, pp. 1494–1502, May 2012.
[20] V. Ignatova, P. Granjon, and S. Bacha, "Space vector method for voltage dips and swells analysis," *IEEE Trans. Power Del.*, vol. 24, no. 4, pp. 2054–2061, Oct. 2009.
[21] N. E. Huang, "Introduction to the Hilbert–Huang transform and its related mathematical problems," *Hilbert–Huang Transf. Appl.*, pp. 1–26, 2014.
[22] Y. Wang, Q. Li, F. Zhou, Y. Zhou, and X. Mu, "A new method with Hilbert transform and slip-SVD-based noise-suppression algorithm for noisy power quality monitoring," *IEEE Trans. Instrum. Meas.*, vol. 68, no. 4, pp. 987–1001, Apr. 2018.
[23] S. Hasan, K. M. Muttaqi, and D. Sutanto, "Detection and characterization of time-variant nonstationary voltage sag waveforms using segmented Hilbert–Huang transform," *IEEE Trans. Ind. Appl.*, vol. 56, no. 4, pp. 4563–4574, 2020.
[24] S. Hasan, K. M. Muttaqi, and D. Sutanto, "Automated segmentation of the voltage sag signal using Hilbert Huang transform to calculate and characterize the phase angle jump," in *Proc. IEEE Ind. Appl. Soc. Annu. Meeting*. IEEE, Sep. 2019, pp. 1–6.
[25] D. S. Laila, A. R. Messina, and B. C. Pal, "A refined Hilbert–Huang transform with applications to interarea oscillation monitoring," *IEEE Trans. Power Syst.*, vol. 24, no. 2, pp. 610–620, May 2009.
[26] Z. Wu and N. E. Huang, "Ensemble empirical mode decomposition: A noise-assisted data analysis method," *Adv. Adapt. Data Anal.*, vol. 1, no. 1, pp. 1–41, 2009.
[27] A. R. Hassan and M. I. H. Bhuiyan, "Computer-aided sleep staging using complete ensemble empirical mode decomposition with adaptive noise and bootstrap aggregating," *Biomed. Signal Process. Control*, vol. 24, pp. 1–10, Feb. 2016.
[28] B. Liu, S. Riemenschneider, and Y. Xu, "Gearbox fault diagnosis using empirical mode decomposition and Hilbert spectrum," *Mech. Syst. Signal Process.*, vol. 20, no. 3, pp. 718–734, Apr. 2006.
[29] Y. Lei, Z. He, and Y. Zi, "EEMD method and WNN for fault diagnosis of locomotive roller bearings," *Expert Syst. Appl.*, vol. 38, no. 6, pp. 7334–7341, 2011.
[30] K. Dragomiretskiy and D. Zosso, "Variational mode decomposition," *IEEE Trans. Signal Process.*, vol. 62, no. 3, pp. 531–544, Feb. 2014.
[31] Q. Ni, J. C. Ji, K. Feng, and B. Halkon, "A fault information-guided variational mode decomposition (FIVMD) method for rolling element bearings diagnosis," *Mech. Syst. Signal Process.*, vol. 164, Feb. 2022, Art. no. 108216.
[32] N. E. Huang, Z. Shen, and S. R. Long, "A new view of nonlinear water waves: The Hilbert spectrum," *Annu. Rev. Fluid Mech.*, vol. 31, no. 1, pp. 417–457, 1999.
[33] J. Wu *et al.*, "A new method for power quality disturbance detection based on improved empirical wavelet transform," *Electr. Power Automat. Equip.*, vol. 40, no. 6, p. 142, 2020.

HEYANG LI was born in Renhuai, Guizhou, China, in 1996. He received the B.E. degree in electrical engineering and its automation from the South China University of Technology, in 2019. He is currently pursuing the master's degree with Xiamen University.

He holds two invention patents on voltage sag detection technology. His research interests include power quality, voltage sag, microgrid control and application, and dynamic voltage restorer.

CHAO MENG (Member, IEEE) was born in Dongping County, Shandong, China, in 1985. He received the B.E. degree in measurement and control technology and instrumentation from the Shandong University of Science and Technology, in 2008, and the Ph.D. degree in mechatronics engineering from Xiamen University, in 2013.

Since July 2013, he has been working as a full-time Research Engineer with the College of Energy, Xiamen University. He has undertaken more than 20 scientific research projects, published more than 20 papers, authorized seven invention patents, and participated in the preparation of three energy and power industry standards. His research interests include advanced power electronic technology and equipment, power quality theory and governance technology, lithium battery energy storage systems, and integrated energy systems, and the number of scientific research results have been successfully industrialized.

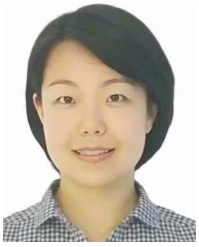

YINGRU ZHAO received the Ph.D. degree in physics from Xiamen University, in 2008.

She was a Postdoctoral Research with Imperial College London, from 2008 to 2011. She is currently the Deputy Dean of the College of Energy, Xiamen University, a Professor, and a Ph.D. Supervisor in energy efficiency engineering. She published more than 50 SCI papers with an H index of 25 and published three translations and participated in the compilation of six Chinese and English books. It has applied for 12 national patents and obtained three software copyrights. Her research interests include energy system engineering, mainly focusing on the optimization design and operation management of complex energy systems, focusing on advanced power cycle, chemical power poly-generation, smart integrated energy, and other application research.

Dr. Zhao serves as a member of the Youth Working Committee of the Engineering Thermodynamics and Energy Utilization Branch of the Chinese Society of Engineering Thermophysics. She was selected for the "Lindao Project" of the German Science Center, in 2008. She was invited by the Lindao Nobel Prize Winners Conference Foundation to attend the 58th Nobel Prize Winners Conference as one of the 25 young Chinese scientists. In 2011, she was selected as the "New Century Excellent Talents Support Program" and "High-Level Overseas Students in Xiamen City" by the Ministry of Education. She won the "Fujian Outstanding Youth Fund," in 2021. She concurrently serves as the Vice Chairman of the Fujian Electrical Engineering Society and the Vice Chairman of the Smart Energy Professional Committee. She has presided over more than 40 projects, including the General and Youth Projects of the National Natural Science Foundation of China, the Sino-German Science Foundation, the National International Science and Technology Cooperation Project, the Fujian Science and Technology Plan Project, the World Bank Project, the U.S. Energy Fund Project, and the projects entrusted by enterprises and institutions. She has won international academic awards, such as Applied Energy Outstanding Paper Award, Schneider Electric 2016 Green Energy Global Innovation Case Challenge, China, and fourth place in the global finals, and won the second prize of China Construction Science and Technology Award. She serves as the Deputy Editor-in-Chief for *Renewable and Sustainable Energy Transitions*, the Editor-in-Chief for *Applied Energy*, *Progress in Energy*, *Smart Energy*, *Scientific Reports*, *Frontiers in Energy Research*, and other international journals, and the Special Editor-in-Chief for the *Global Energy Internet*.